

Resonant Column Apparatus Tests on Intact and Jointed Rock Specimens with Numerical Modelling Validation

A. Perino · G. Barla

Received: 15 October 2013 / Accepted: 24 February 2014 / Published online: 5 April 2014
© Springer-Verlag Wien 2014

Abstract The determination of rock mass dynamic parameters including the influence of joints/discontinuities on wave propagation is of interest for solving problems in geophysics, rock protective engineering, rock dynamics and earthquake engineering. This topic is covered in this paper by means of laboratory tests on intact and jointed rock specimens performed with the resonant column apparatus (RCA). Attention is dedicated to the determination, with this equipment, generally used for testing soils, of the shear modulus at small strain and the damping ratio of intact and jointed rock specimens. A correction procedure based on the RCA tests performed on aluminium specimens is described. The results of the tests performed are analysed in detail. Three-dimensional distinct element method modelling is used to evaluate the applicability of the RCA and the correctness of the laboratory tests performed. A comparison with the results obtained using the scattering matrix method is also presented.

Keywords Rock dynamic · Resonant column apparatus tests · Intact and jointed rock specimens · DEM analyses · Scattering matrix

1 Introduction

The static and dynamic properties of geomaterials can be measured with different types of equipment. In particular, the resonant column apparatus (RCA) is used for testing soils and determining the dynamic properties at low strain

level. It is known that attention is needed with this equipment when the material to test becomes stiffer as discussed by Kumar and Clayton (2007) and Clayton et al. (2009) who showed the influence of the torsional stiffness of the specimen on the RCA results and discussed the effects of the mass and specimen fixity, which produce errors in measuring the resonant frequency.

The interpretation procedure of the experimental results of a fixed-free RCA is based on the theory of elastic wave propagation of a torsional wave. As shown by Drnevich (1978) and Clayton et al. (2009), the shear modulus obtained with the RCA tests can be underestimated due the existence of different patterns of distortion (e.g. the top or the bottom faces of the specimen are not perfectly horizontal, the drive coils are not well matched, or are not accurately aligned or not perfectly connected or driven, or where the magnet polarity is inadvertently reversed during the assembly) and the compliance between the specimen and the RCA and between the drive-system and the platen.

The effects of joints on seismic velocity are to be taken into account when assessing the dynamic properties of rock masses. Several authors have studied this problem with laboratory tests and theoretical methods. Experimental studies focused on the evaluation of the effects of cracks and fractures with different filling conditions, orientation, number, etc. and were carried out by different authors such as Crampin et al. (1980), Aki et al. (1982), Idziak (1988), Pyrak-Nolte and Cook (1987), Pyrak-Nolte et al. (1990a, b), Ekern et al. (1995), Boadu and Long (1996), Kahraman (2002), Leucci (2006), Li and Ma (2009).

Theoretical methods are essentially based on three main approaches. With the first method, as proposed by Fehler (1982), the joint is modelled as a thin plane layer and displacements and stresses are assumed to be continuous across the interfaces. The second method, applied to

A. Perino (✉) · G. Barla
Department of Structural, Geotechnical and Building
Engineering, Politecnico di Torino, Turin, Italy
e-mail: andrea.perino@polito.it

seismic wave propagation by Schoenberg (1980), is the displacement discontinuity method (DDM). The basic assumption is that the particle displacements are discontinuous along a joint while the stresses remain continuous. The third method is the equivalent medium method (EMM), where the jointed medium is represented as a homogeneous one, characterized by effective elastic moduli (e.g. Hudson 1981; Frazer 1990; Coates and Schoenberg 1995; Slawinski 1999; Li et al. 2010).

In this paper, an innovative application of intact and jointed rock specimens testing with the RCA is investigated and specific tests on a soft rock (biocalcarenite) are described. A correction factor (C_F), which depends on the

stiffness of the specimen, is proposed for reducing the errors in the estimate of the shear wave velocity of the rock being tested. This factor is quantified on the basis of RCA tests on aluminium specimens. Also described are the results of simulations of the RCA tests based on distinct element method (DEM) modelling and the scattering matrix method (Perino et al. 2012 and Perino 2011).

2 The Resonant Column Apparatus (RCA)

The resonant column apparatus (RCA) is used to measure the dynamic properties of soils. The basic principle of the

Fig. 1 a, b Views of the resonant column apparatus and c detail of the drive-system

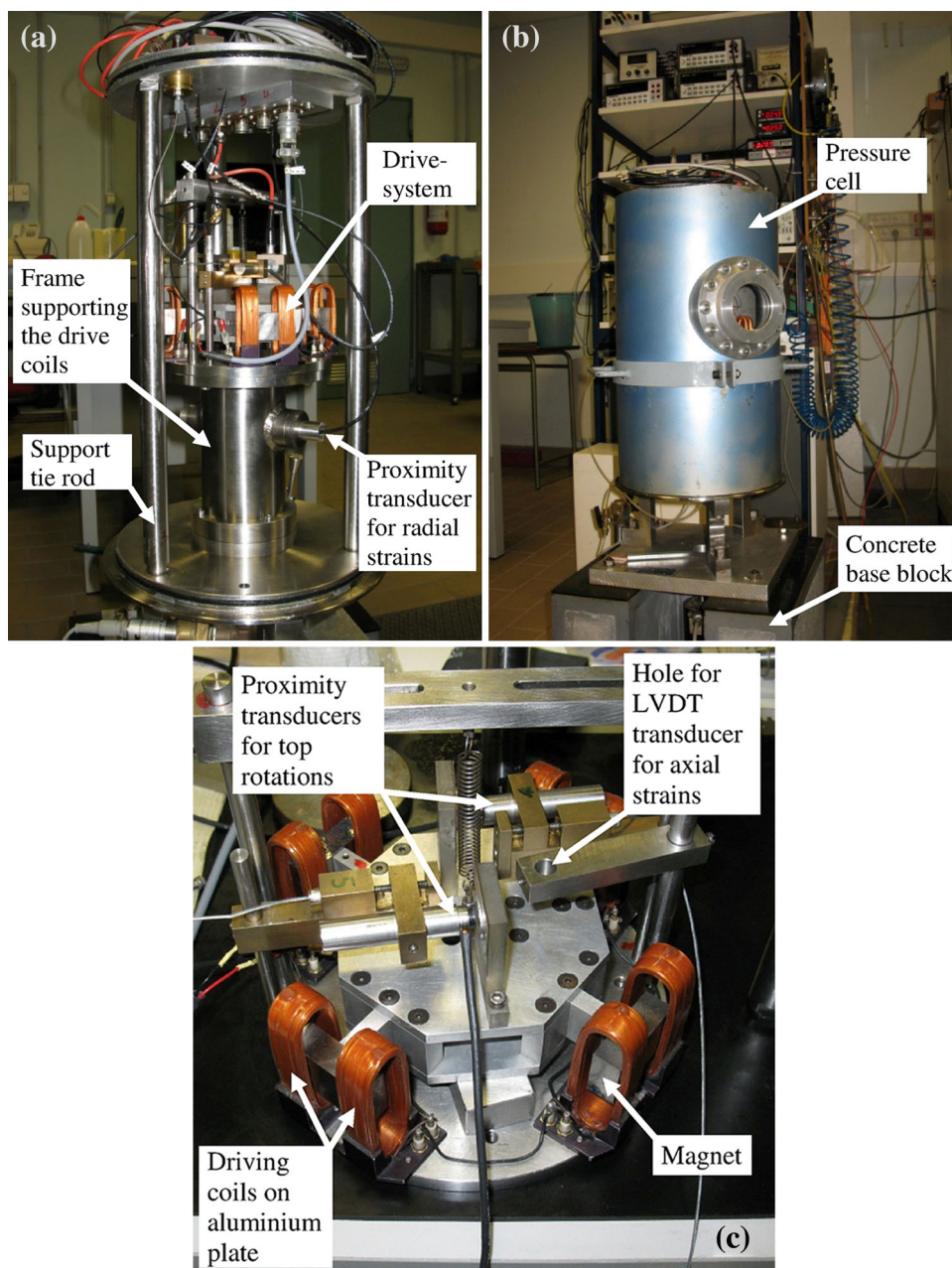
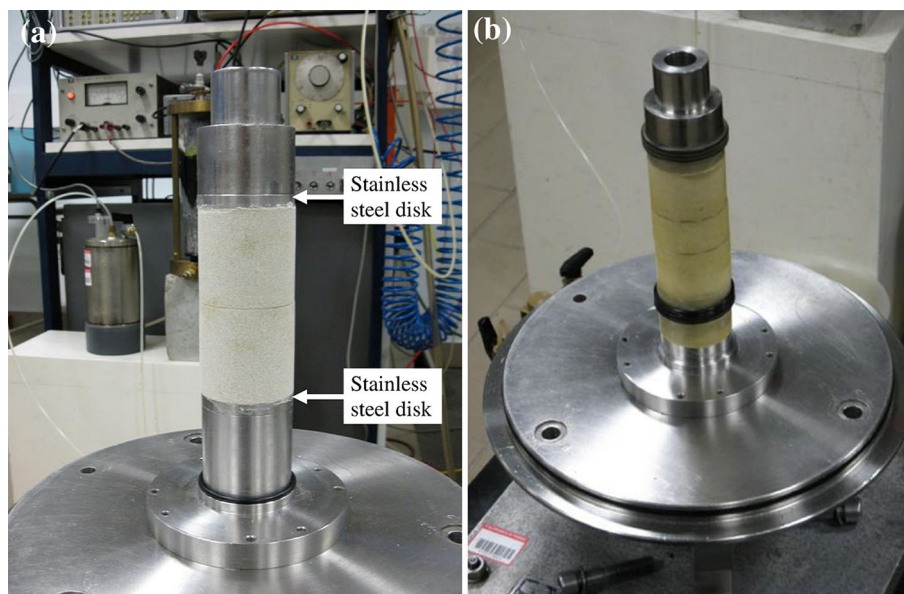


Fig. 2 **a** Detail of the specimen with the ends pasted to the test apparatus and **b** specimen with the membrane placed



test is to vibrate a cylindrical specimen in a fundamental mode of vibration, usually in torsion. Once the fundamental mode is established, measurements of the resonant frequency and of the amplitude of vibration are made.

The shearing strain amplitude during vibration is calculated by measuring the acceleration and frequency of vibration. The wave propagation velocities and the elastic moduli are calculated based on the resonant frequency, specimen size and drive-system mass using the relationships derived from theory of elasticity and torsional wave propagation in cylindrical rods. Viscous damping is determined from the decay of free vibrations.

The RCA used for the tests performed and described in this paper is of the fixed-free type (Fig. 1) with the specimen fixed at the base and free at the top. The excitation system comprises a structure with magnets and coils. These magnets interact with the coils when are crossed with current and transfer to the specimen a cyclic torsion with frequency equal to that of the arrival signal. The response of the system is measured using an accelerometer placed over the head of the specimen in the drive-system.

The RCA for testing soil was modified in order to perform tests on intact and jointed rock specimens. In particular, with the intent to obtain the compliance between the ends of the specimen and the apparatus, the two porous stones generally used for testing soil were substituted with two stainless disks to allow pasting the ends of the specimen (Fig. 2a). In this way, a glued connection between the bottom of the specimen and the base of the apparatus and between the head of the specimen and the top cap was obtained. With the membrane placed around the specimen, o-rings were positioned to fix it to the apparatus (Fig. 2b). The joints, in the tests performed on the jointed rock



Fig. 3 Aluminium specimens tested

specimens, were filled with water to ensure that the membrane did not penetrate into them.

3 Correction Procedure

A correction procedure for the interpretation of the RCA tests is proposed first. This is based on a correction curve obtained with tests performed on nine aluminium specimens each one with a different stiffness. The specimens are shown in Fig. 3, and the geometrical characteristics are given in Table 1. The specimens are formed with two disks at the two ends (diameter 75 mm) and a central rod with diameter ranging from 5 mm minimum to 45 mm maximum.

In the RCA tests, sinusoidal input waves with amplitude between 0.010 and 10.0 V were applied and the resonant frequency was computed accordingly. The sinusoidal input wave contains 20 load cycles and 20 free vibration cycles.

Table 1 Geometrical properties of the aluminium specimens

Specimen	Height of central rod (mm)	Diameter of central rod (mm)	Height of the top and bottom disks (mm)	Diameter of the top and bottom disks (mm)
P1	140	5	5	75
P2	140	10	5	75
P3	140	15	5	75
P4	140	20	5	75
P5	140	25	5	75
P6	140	30	5	75
P7	140	35	5	75
P8	140	40	5	75
P9	140	45	5	75

Each specimen during testing was fixed at the two ends to the drive-system and to the platens with two screws (see the holes in the disks shown in Fig. 3).

The interpretation procedure of the RCA tests (Richart et al. 1970), based on the theory of torsional elastic wave propagation in cylindrical rods, implies the use of the following equations:

$$\frac{I_S}{I_T} = \left(\frac{\omega_n h}{V_S}\right) \cdot \tan\left(\frac{\omega_n h}{V_S}\right) = \beta \cdot \tan \beta \tag{1}$$

$$V_S = \frac{\omega_n h}{\beta} \rightarrow G = \rho V_S^2 \tag{2}$$

where I_S is the mass polar moment of inertia of the specimen, h is its height, $\omega_n (=2\pi f_n)$ is the circular natural frequency and I_T is the mass polar moment of inertia of the steel top cap and of the drive-system. V_S is the shear wave velocity, ρ is the density and G is the shear modulus.

The resonant frequency measured in the resonant column apparatus is the damped natural frequency (ω_d), which is sufficiently close to the natural frequency (ω_n). In this case, the error can be tolerable as ω_d is within 1 % of ω_n . Solving Eq. (1) for β , the shear wave velocity (V_{SAI}) and

the shear modulus of aluminium (G_{Al}) can be found from Eq. (2) as shown in Table 2.

Using the elastic parameters for aluminium $V_{SAI} = 3,172$ m/s and $G_{Al} = 28,368$ MPa obtained with uniaxial compression and ultrasonic tests on aluminium specimens, the correction factor C_F was computed as the ratio of the “correct” shear modulus and the “non-correct” one. The correction curve as shown in Fig. 4 was then derived. It is noted that the error in the estimation of the shear modulus increases with the increasing of the measured resonant frequency.

To verify these results, the resonant frequency of each specimen f_n was computed by assuming the same specimen with the drive-system on the top to be a single degree of freedom system (SDOF):

$$f_n = \frac{1}{2\pi} \sqrt{\frac{k_{Ti}}{I_T}} \tag{3}$$

where I_T is the computed mass polar moment of inertia of the aluminium top cap and the drive-system (44.00 g cm s²) and k_{Ti} is the torsional stiffness of the specimen i given as follows:

$$k_{Ti} = \frac{G_{Al} \left(\frac{\pi D^4}{32}\right)}{h} \tag{4}$$

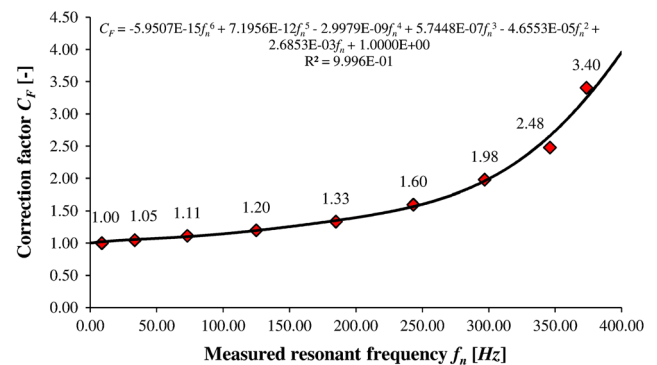


Fig. 4 Correction curve

Table 2 Shear wave velocity and shear modulus obtained from RCA tests on aluminium specimens

Specimen	Inertia sample I_S (g cm s ²)	Inertia RCA I_T (g cm s ²)	β (–)	Resonant frequency f_n (MPa)	Shear wave velocity V_S (m/s)	Shear modulus G (MPa)
P1	2.475e–4	44.0	0.0024	8.54	3,169.39	28,376.00
P2	3.959e–3	44.0	0.0095	33.32	3,098.13	27,114.34
P3	2.004e–2	44.0	0.0213	72.93	3,003.77	25,487.87
P4	6.335e–2	44.0	0.0379	124.79	2,894.18	23,662.07
P5	1.547e–1	44.0	0.0593	184.76	2,743.64	21,264.52
P6	3.207e–1	44.0	0.0853	243.09	2,508.31	17,773.09
P7	5.941e–1	44.0	0.1159	296.73	2,251.90	14,325.09
P8	1.014	44.0	0.1512	345.92	2,013.11	11,448.17
P9	1.624	44.0	0.1909	373.38	1,717.34	8,331.26

Table 3 Resonant frequencies deduced analytically and experimentally

Specimen	Torsional stiffness of the specimen K_{Ti} (Nm)	Computed f_n (Hz)	Measured f_n from RCA (Hz)	Correction factor C_F (–)	Corrected measured f_n from RCA (Hz)	Error between f_n computed and corrected (%)
P1	0.13	8.54	8.54	1.00	8.54	0.00
P2	2.07	34.17	33.32	1.05	34.08	0.25
P3	10.46	76.88	72.93	1.11	76.93	–0.08
P4	33.07	136.67	124.79	1.20	136.63	0.03
P5	80.75	213.54	184.76	1.33	213.40	0.07
P6	167.43	307.50	243.09	1.60	307.12	0.13
P7	310.19	418.55	296.73	1.98	417.57	0.23
P8	529.18	546.67	345.92	2.48	544.53	0.39
P9	847.64	691.88	373.38	3.40	688.99	0.42

Table 4 Physical properties of the Diamante Bateig stone

Physical properties	
Porosity (%)	17.79
CaCO ₃ (%)	>87
MgCO ₃ (%)	>1
Absorption coefficient (ASTM stone testing) ^a (%)	5.8
Density (kg/m ³)	2,169

^a The absorption test (ASTM stone testing) measures the degree to which water will penetrate a stone, measured at a weight percentage

where D and h are the diameter and the height (=140 mm) of the central rod, respectively.

Table 3 gives the resonant frequencies obtained analytically and derived using the correction procedure. It is concluded that the “correct” frequency from the RCA test can be computed by multiplying the “non-correct” value by ($\sqrt{C_F}$). It is noted that this comparison would not be satisfied without a perfect coupling between the specimen, the drive-system and the platen.

4 Rock Tested and Specimens Used

Resonant column apparatus tests were performed on rock specimens of “Diamante Bateig stone”. This rock is a biocalcarene extracted in the Alicante Province (Spain), used as ornamental stone in new-buildings construction and as cladding for existing buildings. It is a nearly homogeneous and isotropic material. The physical properties are summarized in Table 4.

This biocalcarene is rich in foraminifers (mainly Globigerinae) ranging in size from 0.2 to 0.5 mm. Foraminifera shells are generally filled with glauconite and/or siliceous cement. The terrigenous fraction comprises quartz, feldspars, micas, dolostone and other rock fragments. Both the inter-particle and intra-particle porosities vary. The most abundant type of cement present is calcite spar equant-equicrystalline mosaics.

Table 5 Mechanical properties of the Diamante Bateig stone

Mechanical properties	
Uniaxial compressive strength (MPa)	42.1
Tangent Young’s modulus (MPa)	15,316
Average Young’s modulus (MPa)	15,615
Secant Young’s modulus (MPa)	18,302
Poisson ratio (–)	0.24
P-wave propagation velocity (m/s)	3,780

Uniaxial compression and ultrasonic tests were performed on five intact rock specimens to obtain the rock static and dynamic elastic parameters. The uniaxial compression tests, under radial strain controlled conditions, allowed one to obtain the Young’s modulus and the Poisson’s ratio. The ultrasonic tests were performed with the ultrasonic pulse technique method to obtain the P-wave velocity. The mechanical parameters obtained are given in Table 5.

Intact and jointed rock specimens were prepared for the RCA tests as follows:

- A : intact cylindrical specimens with height 100 mm and diameter 50 mm (Fig. 5a);
- B: cylindrical specimens with smooth joints (Fig. 5b, c, d);
- C: cylindrical specimens with toothed joints (Fig. 6)

The B specimens contain one, two or three parallel smooth joints (B1, B2 and B3). The C specimens contain one or two toothed joints (C1 and C2) with the following geometrical characteristics: height of teeth: 1.5 mm; spacing between teeth: 6 mm; width of teeth: 5 mm; contact width of the tooth: 1 mm.

5 RCA Tests on Intact Rock Specimens

In the RCA tests, a sinusoidal torque was applied at the head of the specimen. The amplitude was kept constant

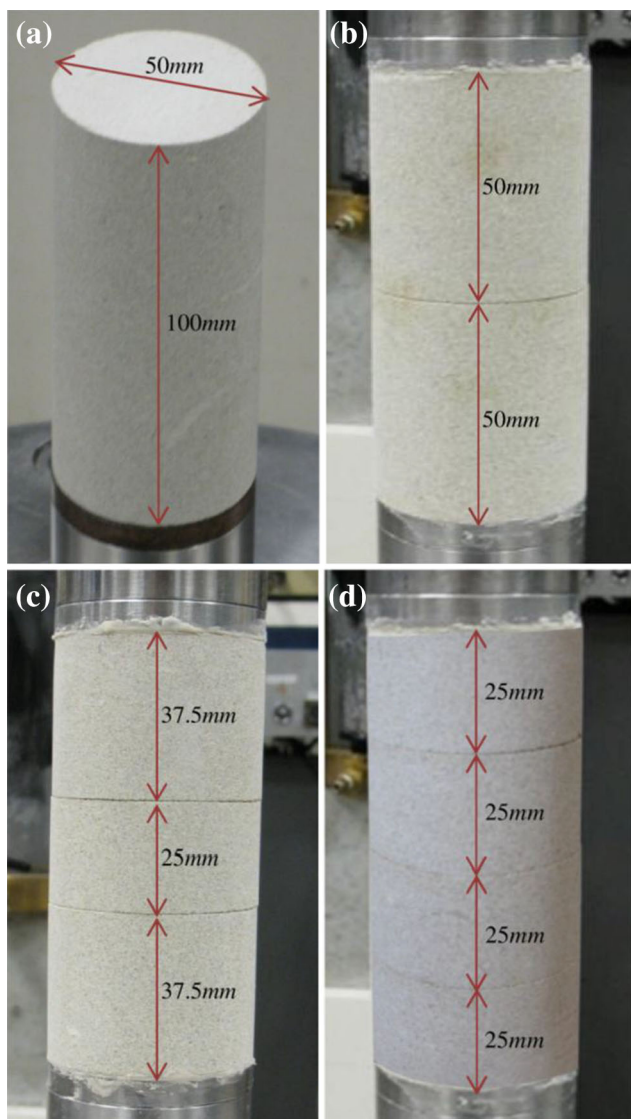


Fig. 5 Intact specimen **a** and specimens with smooth joints (**B**): **b** specimen B1, **c** specimen B2 and **d** specimen B3

while the frequency was changed to find the resonant frequency of the system. The electrical signal applied and the corresponding torsional moment generated are shown in Fig. 7. The input motion comprises a cycle of rest, 20 load cycles and 20 free vibration cycles.

The measured transfer function obtained with the resonant column test for the intact specimen is shown in Fig. 8. A fitting curve is drawn to define more accurately the resonant frequency f_n which results to be about 374 Hz. The RCA tests were repeated four times to check the repetitiveness of the experimental results.

Using the interpretation procedure described in paragraph 3 above [Eqs. (1) and (2)], the shear wave velocity (V_S) and the shear modulus of biocalcarenite (G) are found to be as follows:

- $V_S = 1,268.2$ m/s
- $G = 3,489.0$ MPa ($\gamma = 1.56 \times 10^{-4}$ %)

It is of interest to compare these values of V_S and G , based on the RCA tests, with those obtained with the uniaxial compression and ultrasonic tests (Table 5). It is known that the dynamic Poisson's ratio (ν_d) and the dynamic Young's modulus (E_d) can be calculated using the theory of elasticity as follows:

$$\nu_d = \frac{(V_P/V_S)^2 - 2}{2[(V_P/V_S)^2 - 1]} \quad (5)$$

$$E_d = \rho V_P^2 \frac{(1 - 2\nu_d)(1 + \nu_d)}{(1 - \nu_d)} \quad (6)$$

If the dynamic Poisson's ratio is taken to be equal to the static value ($\nu_d = 0.24$), using the P-wave velocity from the ultrasonic tests ($V_P = 3,780$ m/s), Eq. (5) gives for the shear wave velocity $V_S = 2,220$ m/s. Similarly, Eq. (6) gives the dynamic Young's modulus $E_d = 26,294$ MPa, from which the shear modulus $G = 10,602$ MPa is computed. It is found that both the shear wave velocity and the shear modulus based on the RCA test are greatly underestimated.

At this point, we can use the correction curve to correct the elastic parameters obtained from the RCA tests. As previously mentioned, the shear wave velocity and shear modulus for biocalcarenite are, respectively, equal to 1,268.2 m/s and to 3,489.0 MPa ($\gamma = 1.56 \times 10^{-4}$ %). The correction factor C_F can be defined by entering in the correction curve (Fig. 4) with the measured resonant frequency $f_n = 374$ Hz, to obtain C_F equal to 3.26. Hence, the corrected V_S and G can be computed to be as follows:

$$V_{S_corrected} = V_S \cdot \sqrt{C_F} = 2,289.5 \text{ m/s} \quad (7)$$

$$G_{corrected} = G \cdot C_F = 11,370.1 \text{ MPa}$$

Therefore, it is shown that the error in the determination of V_S with the RCA is significantly reduced.

Another parameter that can be computed from the RCA tests is the material damping ratio D . This was calculated using the half-power bandwidth method and the amplitude decay method.

The half-power bandwidth method requires one to compute the frequencies f_1 and f_2 for which the amplitude of the response spectra (Fig. 8) is $1/\sqrt{2}$ times the amplitude at the resonance frequency f_n . In this case, the material damping ratio is 2.941 %, computed with $f_1 = 362.5$ Hz and $f_2 = 384.5$ Hz.

On the other hand, the amplitude decay method allows one to compute the damping ratio from the attenuation of free vibrations. Figure 9a shows the recorded free vibration decay response curve and the diagram used to compute the logarithmic decrement δ equal to the slope of the

Fig. 6 Views of **a** specimen C1 and **b** specimen C2; **c**, **d** details of the tooth joint

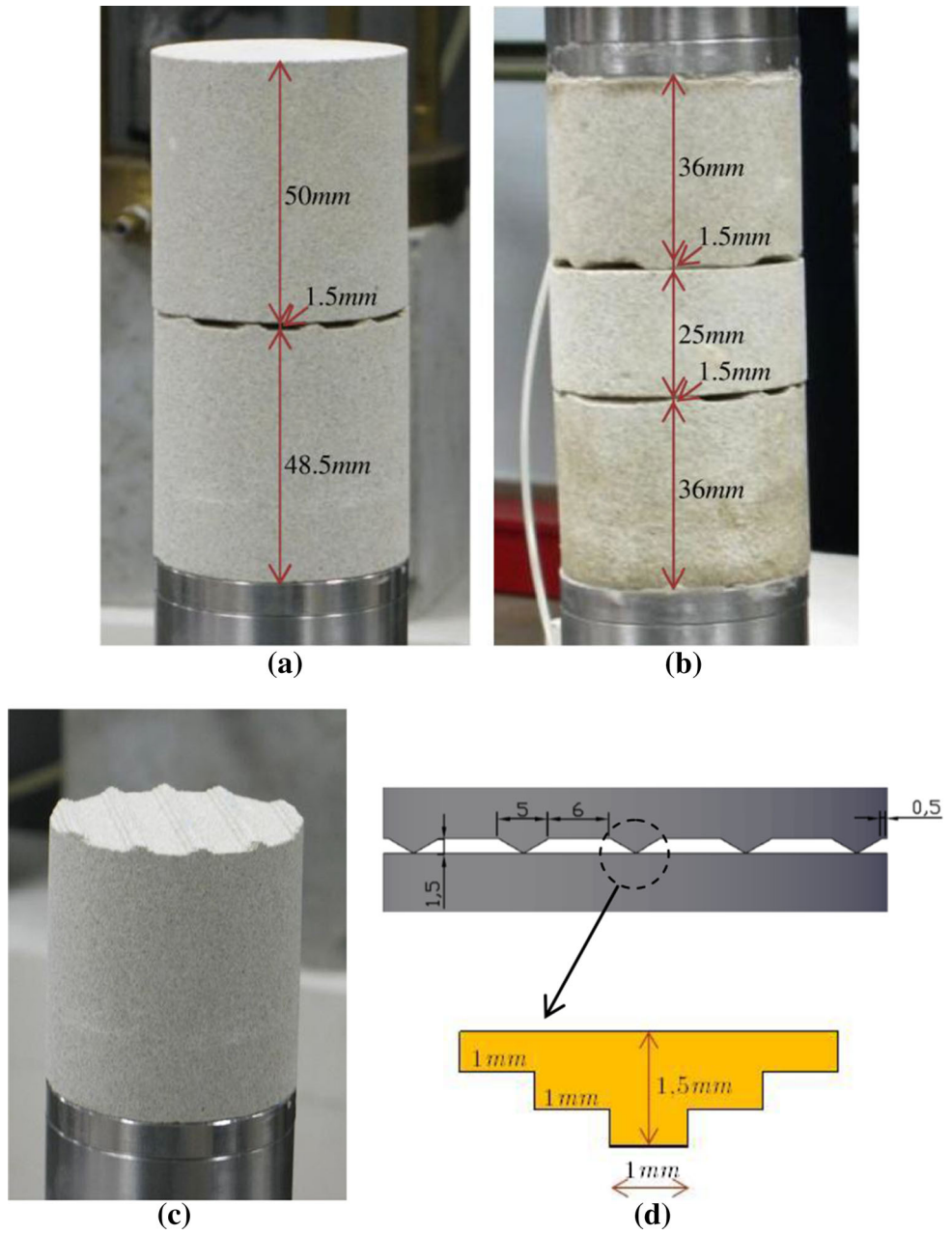
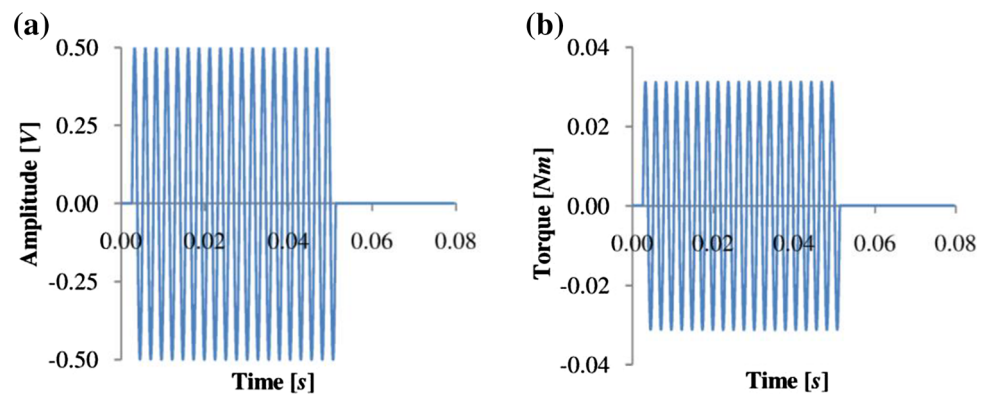


Fig. 7 Torsional wave applied to the head of the specimen: **a** electrical signal in V and **b** torque in Nm



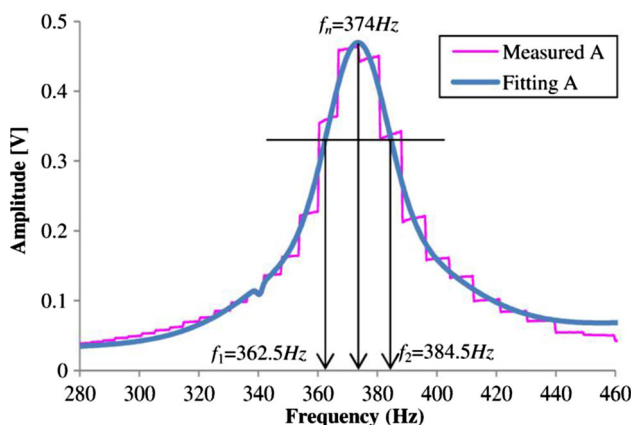


Fig. 8 Measured transfer function for intact specimen A

line of best fit through the data points (Fig. 9b). The material damping ratio obtained from the decrement $\delta = 0.1561$ is 2.484 %. The damping ratio derived with the two methods is similar, and it is characteristic of the rock type tested.

6 RCA Tests of Jointed Rock Specimens

The RCA tests of jointed rock specimens were performed with the same procedures as described for the tests on the intact rock specimen. Figure 10 gives the measured transfer function for the jointed rock specimens with smooth surfaces compared with the measured transfer function for the intact rock specimen.

It is shown that the resonant frequency of the jointed rock specimens decreases with the increase in the number of joints. This decrease is essentially due to the decrease in the specimen stiffness. In fact, the resonant frequency of a specimen in the RCA subjected to torsional excitation is mainly dependent on its torsional stiffness and on the mass polar moment of inertia of the top cap and the drive-system.

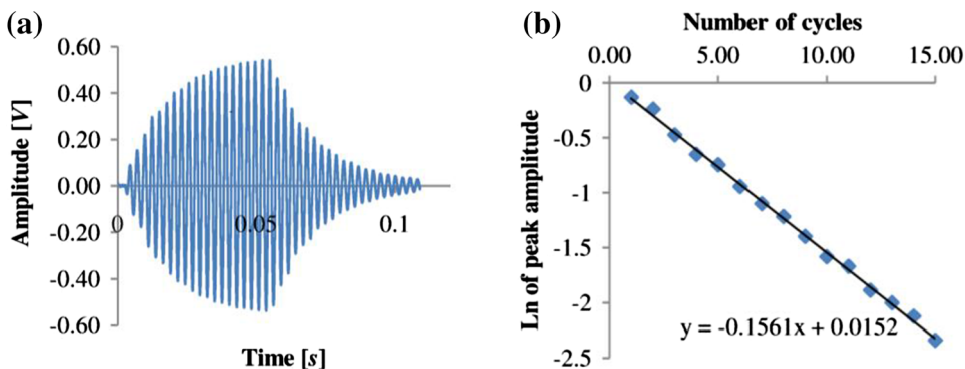
This holds true provided that the compliance condition between the specimen and the apparatus is verified, which is easily proven since the effect of a joint in the intact specimen causes a decrease in torsional stiffness and then a decrease in the resonant frequency and an increase in the amplitude of the transfer function. The amplitude of the transfer function increases with the increase in the number of joints, with the consequence that the rotation on the head of the specimen increases.

The resonant frequencies and the shear wave velocities of each specimen are summarized in Table 6. It is noted that the classical procedure to compute the shear wave velocity in the RCA tests was used also for the jointed rock specimens and that each test in the RCA was repeated four times. A confining pressure of 100 kPa was applied to maintain the specimen in place.

Difficulties were found when testing the C2 specimen, essentially due to the irregularities of the contact between the joint surfaces which caused small movements affecting the results. The measured resonant frequency for this specimen was found to be greater than that of the intact rock specimen, which is clearly not possible. This is due to the fact that the torque applied does not mobilize all the parts of the specimen because the joints very likely do not allow the transmission of motion. In fact, the upper parts of the C2 specimen (Fig. 6b) can rotate on the part fixed on the base of the RCA and do not transmit the torsional wave. This generates an increase in the resonant frequency and then of the stiffness of the system. This increase is only possible if the height of the equivalent SDOF system decreases and this proves that probably the fixed part of the specimen on the base of the resonant column is not mobilized.

Based on the correction factor C_F given in Fig. 4, the correct values of the shear wave velocity were derived as shown in Table 6. Then, the decay of the response, recorded at the top of the specimen, was evaluated. The damping ratio computed for specimens with smooth joints is 3.96 % for B1, 4.03 % for B2 and 3.62 % for B3. On the other hand, the damping ratio for the C2 specimen is about 2.76 %.

Fig. 9 Computation of the logarithmic decrement: **a** free vibration decay response curve; **b** the slope of the least-squares regression line fitted to the data provides the logarithmic decrement δ



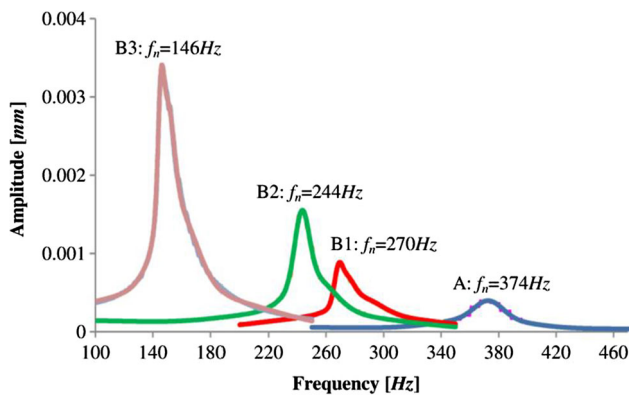


Fig. 10 Measured transfer functions for intact and jointed specimens

Table 6 Shear wave velocities from RCA tests

Specimen	Resonant frequency f_n (Hz)	Shear wave velocity V_S (m/s)	Correction factor C_F (-)	Corrected shear wave velocity V_S (m/s)
A	374	1,268.2	3.26	2,289.9
B1	270	913.2	1.73	1,201.1
B2	244	825.2	1.57	1,034.0
B3	146	490.1	1.25	547.9
C1	194	656.1	1.38	770.8
C2	388	-	-	-

By comparing the damping ratio of the intact rock specimen, the part of energy attenuation (2.48 %) due to the presence of joints can be found. However, it is not easy to evaluate, from these results, the influence of a single joint on the attenuation of energy. In all cases, it is shown that the damping ratio increases from the intact rock specimen to the jointed one.

7 DEM Modelling

The distinct element method (DEM) was used together with the RCA tests with the following main objectives:

1. To assess the correction procedure proposed for the interpretation of the RCA tests when stiff geomaterials (i.e. a soft rocks, as in this paper) are used;
2. To simulate the RCA testing of the intact rock specimens;
3. To simulate the RCA testing of the jointed rock specimens.

The DEM and the 3DEC code (Itasca Consulting Group, Inc, USA) were used. The purpose of each model was to mimic as closely as possible the RCA during testing. The

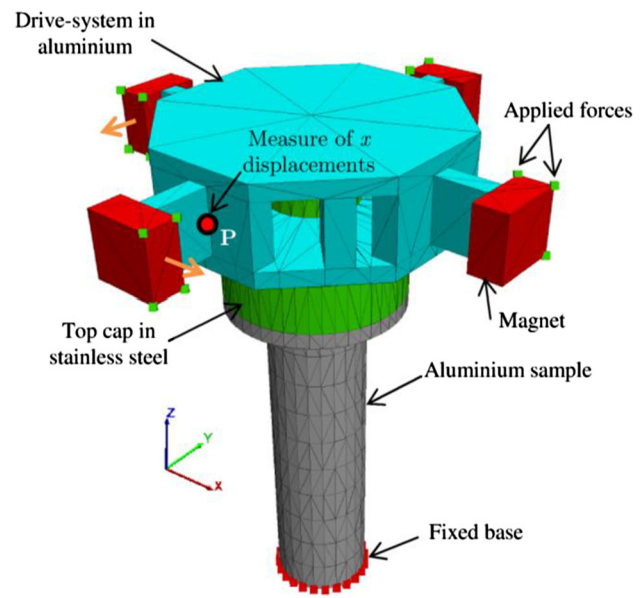


Fig. 11 3DEC model of the resonant column with the aluminium specimen P8

numerical analyses were performed by simulating the testing procedure adopted in the laboratory tests previously described and by creating suitable DEM models. The mesh element size was assumed lower than 1/10 of the wavelength of the propagating wave, in accordance with Kuhlemeyer and Lysmer (1973). The head of the specimen was joined with the drive-system, while the bottom was fixed in all directions.

The excitation was generated by forces applied at each node of the blocks forming the magnets. Forces were computed by dividing the torque applied in the laboratory tests (Fig. 7) for the distance between the point of force application and the axis of rotation. A Rayleigh material damping was assumed based on the damping ratio obtained in the RCA tests.

7.1 Assessment of the Correction Procedure

A DEM model of the RCA with the aluminium specimen included is illustrated in Fig. 11, where linear elastic joined deformable blocks were used. Values of the natural frequency of oscillation of the model were calculated by recording the horizontal displacements at the top versus time. The comparison with the measured response of the system was possible with the unit conversion of the accelerometer recorded amplitudes. This conversion can be performed through the computation of the rotation of the head of the specimen as follows:

$$\vartheta = \frac{\Delta a}{r_a} = \frac{\sqrt{2} \cdot a \cdot g}{(2\pi f)^2 \cdot ACF \cdot r_a} \tag{8}$$

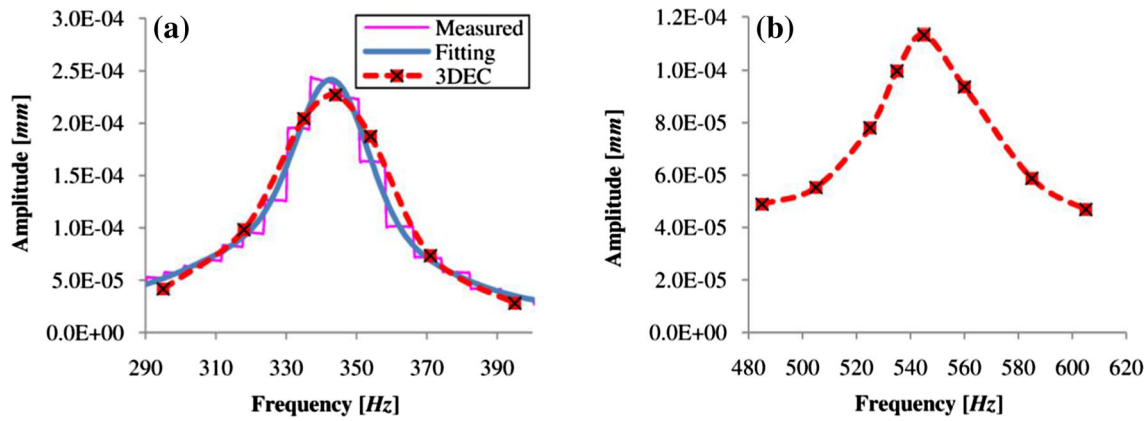


Fig. 12 Transfer function computed with 3DEC code with measured (a) and corrected (b) elastic parameters for the specimen P8

Table 7 Resonant frequencies computed with 3DEC code for aluminium specimens

Specimen	f_n from 3DEC with uncorrected parameters (Hz)	f_n from 3DEC with corrected parameters (Hz)
P1	8.90	8.91
P2	33.41	33.83
P3	73.50	76.93
P4	126.10	138.01
P5	187.85	215.21
P6	246.31	309.23
P7	297.20	418.55
P8	347.01	546.67
P9	375.71	690.20

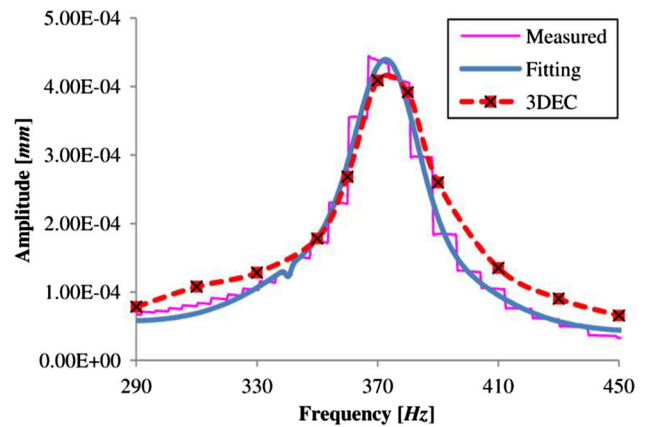


Fig. 14 Measured and numerical transfer function for intact specimen A

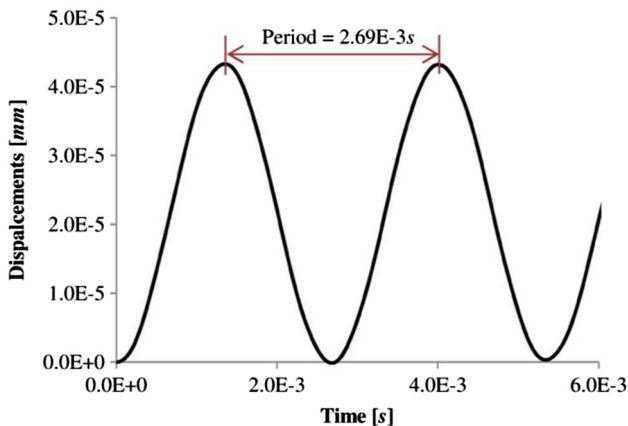


Fig. 13 Plot of horizontal displacements versus time recorded at the top of the 3DEC model for the intact specimen A

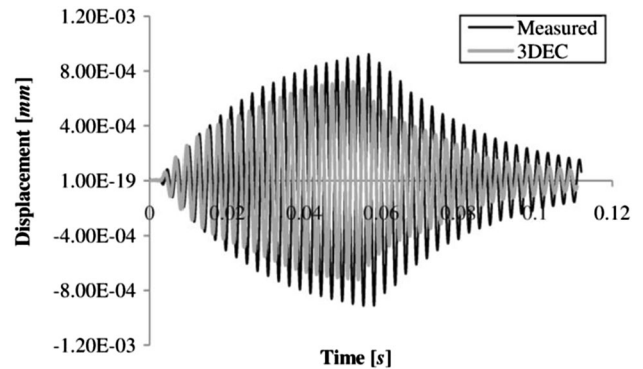


Fig. 15 Measured and DEM responses at the resonant frequency for the specimen A

where Δa is the displacement of the accelerometer, a is the root-mean-square acceleration amplitude obtained from the acceleration measurements of the accelerometer, ACF is the calibration factor of the accelerometer = 2,500 pk-mv/

pk-g, r_a is the radial distance between the axis of rotation and the point in which the accelerometer is located in the laboratory apparatus (=50 mm).

The displacements measured in the laboratory tests were computed as follows:

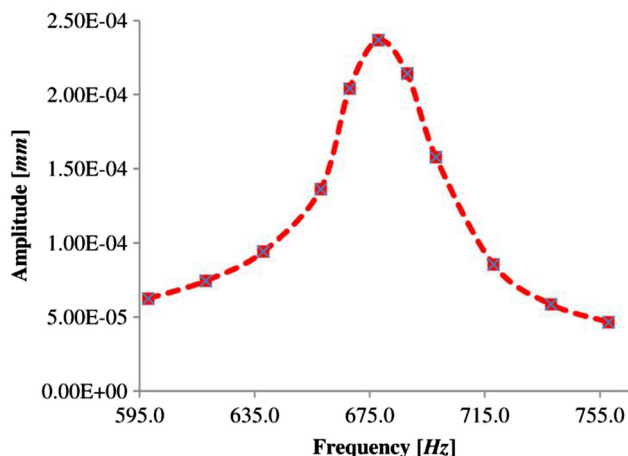


Fig. 16 Numerical transfer function for intact specimen A obtained with the corrected mechanical parameters of the rock

$$\Delta x = r \cdot \vartheta^{\text{rad}} \tag{9}$$

where $r = 55 \text{ mm}$ is the distance between the axis of rotation and point P (Fig. 11).

As example, Fig. 12 shows the transfer function obtained for the P8 specimen, with the elastic parameters derived from the RCA tests and corrected with the correction curve. Values of the resonant frequencies computed with 3DEC for all aluminium specimens by assuming uncorrected and corrected elastic parameters of the

material are summarized in Table 7. It is shown that the resonant frequencies obtained with the DEM analyses are very close to those measured in the RCA and then corrected according to the proposed correction procedure.

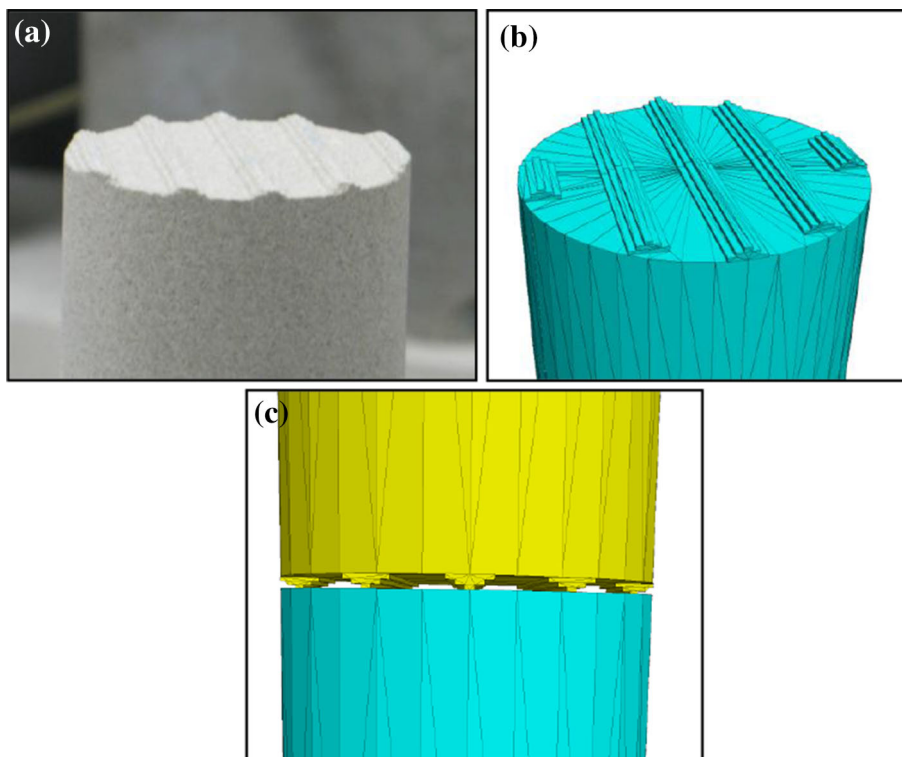
7.2 Simulation of RCA Testing of Intact Rock Specimen

The DEM model of the RCA is the same of that shown in Fig. 11 except for the aluminium specimen that was replaced with the intact rock specimen. Linear elastic joined deformable blocks were used for discretization. To calibrate the model, gravity was applied to the resonant column in the horizontal direction and the natural frequency of the system was computed, which must be nearly equal to the experimental resonant frequency.

The analyses were performed with the material damping assumed to be zero. Values of natural frequency of oscillation were calculated by recording the horizontal displacements at the top (P in Fig. 11) of the model versus time. The recorded time history for the intact rock specimen is shown in Fig. 13, where the period of oscillation is $2.69 \times 10^{-3} \text{ s}$ and the natural frequency is 372 Hz.

A comparison between the measured transfer function and that obtained with the DEM model is shown in Fig. 14. Similarly, the decay of the response at the top of the specimen, obtained with the laboratory test and the numerical model, is depicted in Fig. 15. It is clear that the

Fig. 17 Details of the joint modelling: **a** real specimen, **b**, **c** DEM model



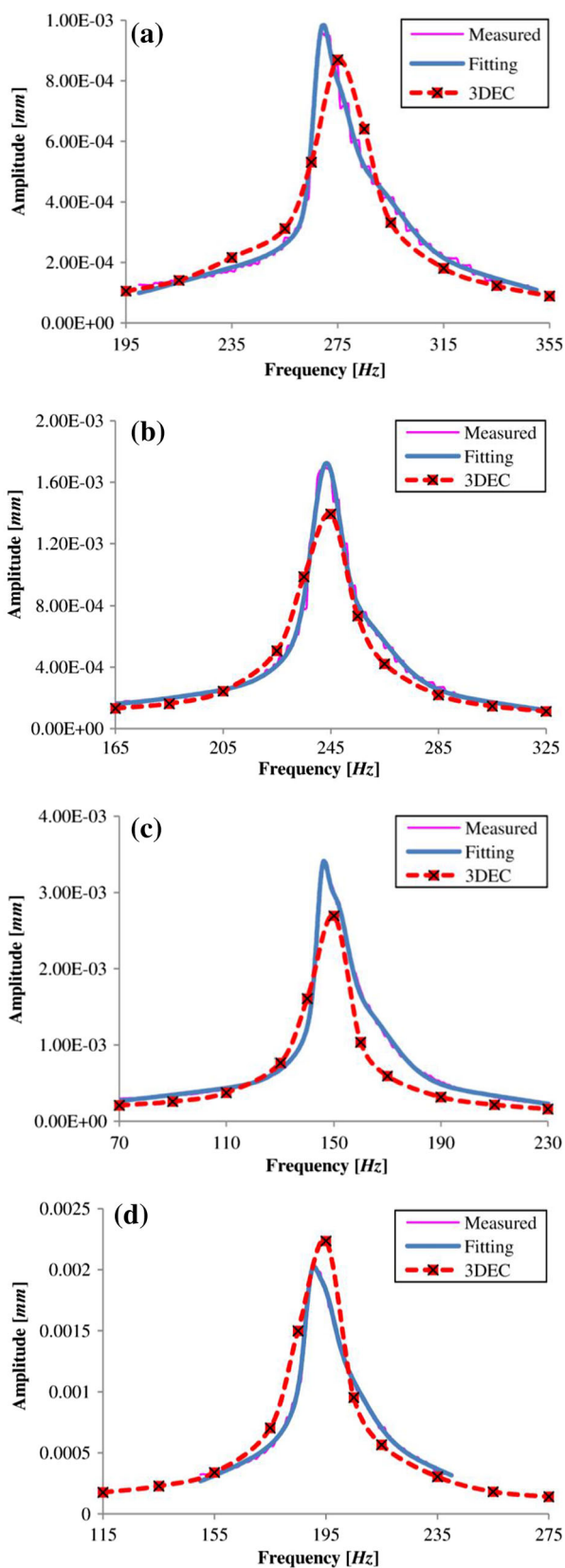


Fig. 18 Measured and numerical transfer function for jointed specimens **a** B1, **b** B2, **c** B3, **d** C1

DEM results well reproduce the laboratory data, and the decay of the response curve is essentially the same. This can also be noted in Fig. 14, where the width of the spectra, at $1/\sqrt{2}$ of the maximum amplitude, obtained in the laboratory is similar to that derived with the DEM analyses.

Finally, the simulated transfer function derived from the DEM model with the elastic parameters corrected with the correction procedure is plotted in Fig. 16. The frequency obtained by the DEM analysis is 678 Hz, which is very close to the value measured during the RCA test ($f_n \cdot \sqrt{C_F} = 374 \cdot \sqrt{3.26} = 675.3$ Hz).

7.3 Simulation of RCA Testing of Jointed Rock Specimens

The DEM intact rock specimen model was also used for the jointed rock specimens model, with joints being introduced in addition to the linear elastic joined deformable blocks. The Rayleigh material damping was estimated from the RCA tests. Figure 17 shows a detail of the model of the toothed rock specimens C1 and C2. The joints in the DEM model were assumed to follow a linear elastic behaviour.

The normal and shear joint stiffnesses were computed from the results of the RCA tests. For example, the joint shear stiffness can be obtained from the measured resonant frequency of the intact specimen and that of the jointed one. The stiffness of a joint (k_J) can be estimated as:

$$\frac{1}{k_{Js}} = \frac{1}{k_{int}} + \frac{i}{k_J} \rightarrow k_J \quad (10)$$

where k_{Js} is the torsional stiffness of the jointed rock specimen (e.g. B1), k_{int} is the torsional stiffness of the intact rock specimen, i is the number of joints and k_J is the joint stiffness.

The resonant frequency obtained with DEM for a jointed rock specimen was found to be the same as that computed with an intact rock specimen with equivalent stiffness k_{Js} . In fact, the DEM analyses, e.g. for specimen B1, show that the resonant frequency computed is the same as that obtained with the intact rock specimen model where the equivalent elastic constants are estimated from the RCA tests.

These considerations prove that the jointed rock specimen remains in the linear elastic field during the RCA test. The comparison between the measured and the computed transfer functions plotted in terms of horizontal displacement is shown in Fig. 18. Moreover, the damping ratio of the laboratory tests and the numerical analyses is essentially the same.

The DEM analyses also show that all the parts of the jointed rock specimens are mobilized. It is noted that this is not the case for the C2 specimen. For example, the

distribution of the horizontal displacements in the B2 specimen (Fig. 5c), evaluated at an instant of time during the simulation of the RCA test, is shown in Fig. 19. The discontinuity of displacements along the joints, assumed in most analytical methods to evaluate the effects of the joints on wave propagation, is well described (e.g. the scattering matrix method (SMM) by Perino et al. 2012 and Perino 2011).

Finally, DEM analyses were performed with the corrected elastic parameters of biocalcarenite [Eq. (7)] estimated with the correction procedure for all jointed specimens. The simulated transfer function obtained for the B1 specimen is plotted in Fig. 20. Table 8 gives a summary of the results obtained for all the specimens. It is shown that the resonant frequencies given by the DEM analyses using the corrected mechanical parameters agree well with the resonant frequencies estimated with the correction curve.

8 Wave Velocity Reduction

It is known that joints generate an attenuation effect which increases with the increasing in the number of joints (Fig. 10; Table 6). Moreover, when a wave crosses a joint a group time delay is originated and a velocity dispersion phenomenon occurs. The phase and the group velocities are equivalent in an elastic half-space. Hence, the velocity dispersion can be computed from the ratio between the effective velocities and the intact group velocity (V_S).

The effective shear wave velocity for the B1 specimen is 47.5 % smaller than the intact group velocity (V_S). The corresponding values for B2 and B3 are 54.8 and 76.1 %, respectively. The dispersion of the shear wave velocity can also be estimated with the analytical approach proposed by Pyrak-Nolte and Cook (1987) or with the SMM (Perino et al. 2012 and Perino 2011).

Unlike the procedure proposed by Pyrak-Nolte and Cook (1987), the SMM considers all multiple reflections in the evaluation of the time delay due to the joints. The first step in this approach is the computation of the phase shift Θ_T of the transmission coefficient T_N obtained for a set of N joints:

$$\Theta_T(\omega, \vartheta) = \text{angle}(T_N) \tag{11}$$

where ω is the angular wave frequency and ϑ is the angle of incidence of the elastic wave. T_N is function of the medium impedance (ρV_S), the joint stiffness and the frequency (Perino et al. 2012).

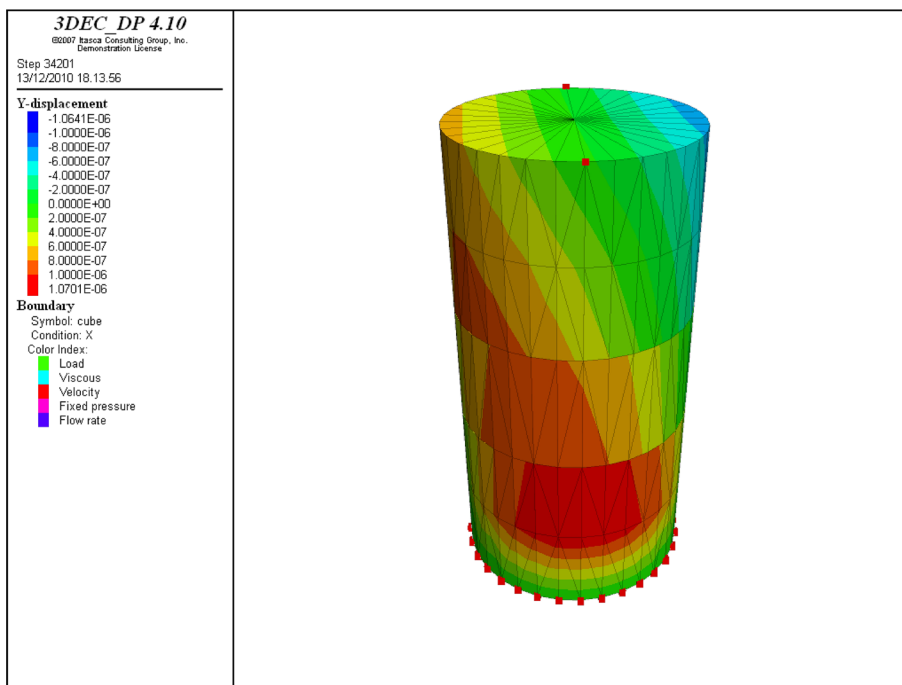
The second step is the evaluation of the group time delay due to the joints (t_{joint}) for the transmitted wave as follows.

$$t_{\text{joint}}(\omega, \vartheta) = \frac{d\Theta_T}{d\omega} \tag{12}$$

The effective shear wave velocity ($V_{S,\text{eff}}$) is obtained from the effective group travel time (t_{eff}):

$$t_{\text{eff}}(\omega, \vartheta) = \frac{l_i / \cos \vartheta}{V_g} + t_{\text{joint}}(\omega, \vartheta) \rightarrow V_{S,\text{eff}}(\omega, \vartheta) = \frac{L / \cos \vartheta}{t_{\text{eff}}} \tag{13}$$

Fig. 19 Discontinuity of horizontal displacements in the specimen B2 evaluated in an instant of time of DEM resonant column analysis



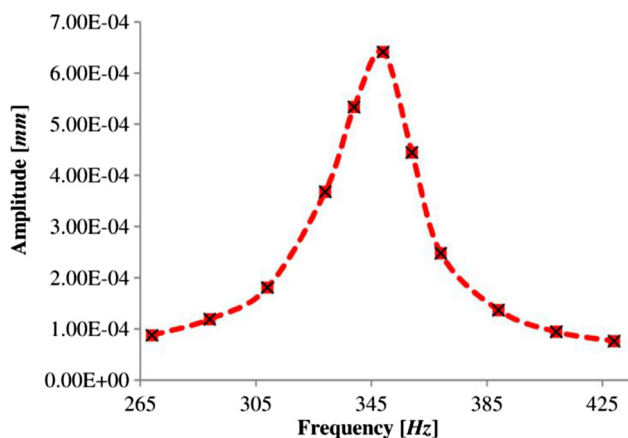


Fig. 20 Numerical transfer function for jointed specimen B1 obtained with the corrected mechanical parameters of the rock

Table 8 Uncorrected and corrected resonant frequencies obtained from RCA laboratory tests and from 3DEC analyses

Specimen	Uncorrected resonant frequency from RCA (Hz)	Correction factor C_F (-)	Corrected resonant frequency from RCA (Hz)	Corrected resonant frequency from 3DEC (Hz)
A	374	3.26	675	678
B1	270	1.73	355	349
B2	244	1.57	306	302
B3	146	1.25	163	158
C1	194	1.38	228	220

where l_i is the travelled distance normal to the joints before the first and after the last joint from the ends of the specimen of length L , V_g is the group velocity of the intact homogeneous isotropic rock ($=V_S$). Here, $V_{S,eff}$ is computed for a rock with joints with the assumption that no dispersion in the intact part of rock is developed.

The results based on Eq. (13) are obtained by assuming the joint shear stiffness used in the DEM analyses and L taken to be equal to the height of the specimens (100 mm). The frequencies investigated are the resonant frequencies deduced experimentally for various types of specimens. The results obtained with SMM and RCA tests are summarized in Table 9, where the effective wave velocity is shown to be frequency and joint stiffness dependent.

9 Conclusions

With the resonant column tests on intact and jointed rock specimens, as described in this paper, an attempt was made

Table 9 Rate in decrease of the shear wave velocity

Specimen	RCA (%)	SMM (%)
B1	47.5	48.6
B2	54.8	65.3
B3	76.1	73.9

to see whether the resonant column apparatus (RCA) is applicable to test intact and jointed rock specimens and to assess the influence of joints on wave propagation. DEM modelling was also used as a means for validating the experimental results.

It was found that, using the correction procedure described in this paper, the shear modulus and the shear wave velocity for stiff materials, such as soft rocks, can be measured. It was also found that the underestimation of these parameters increases with the increasing in the measured resonant frequency. Also, the influence of joints on wave propagation was well demonstrated.

References

- Aki K, Fehler M, Aarmodt RL, Albright JN, Potter RM, Pearson CM, Tester JW (1982) Interpretation of seismic data from hydraulic fracturing experiments at the Fenton Hill, New Mexico, Hot Dry Rock. *J Geophys Res* 87:936–944
- Boadu FK, Long TL (1996) Effects of fractures on seismic wave velocity and attenuation. *Geophys J Int* 127:86–110
- Clayton CRI, Priest MB, Zervos A, Kim SG (2009) The Stokoe resonant column apparatus: effects of stiffness, mass and specimen fixity. *Geotechnique* 59(5):429–437
- Coates RT, Schoenberg M (1995) Finite-difference modeling of faults and fractures. *Geophysics* 60:1514–1526
- Crampin S, McGonigle R, Bamford D (1980) Estimating crack parameters from observation of P-wave velocity anisotropy. *Geophysics* 45:361–375
- Drnevich VP (1978) Resonant column testing: problems and solutions. In: Silver ML (ed) *Dynamic geotechnical testing*, ASTM STP 654. West Conshohocken, PA, ASTM International, pp 384–398
- Ekern A, Suarez-Rivera R, Hansen A (1995) Investigation of interface wave propagation along planar fractures in sedimentary rocks. In: Daemen JJK, Schulz R (eds) *Proceedings of the 35th US symposium on rock mechanics*. A.A. Balkema, Rotterdam, Lake Tahoe, CA, pp 161–167
- Fehler M (1982) Interaction of seismic waves with a viscous liquid layer. *Bull Seism Assoc Am* 72:55–72
- Frazier LN (1990) Dynamic elasticity of microbedded and fractured rocks. *J Geophys Res* 95:4821–4831
- Hudson JA (1981) Wave speeds and attenuation of elastic waves in material containing cracks. *Geophys J R Astron Soc* 64:133–150
- Idziak A (1988) Seismic wave velocity in fractured sedimentary carbonate rocks. *Acta Geophys Pol* 36:101–114
- Kahraman S (2002) The effects of fracture roughness on P-wave velocity. *Eng Geol* 63:347–350
- Kuhlemeyer R, Lysmer J (1973) Finite element method accuracy for wave propagation problems. *J Soil Mech Found Div, ASCE*. 99. SM5: 421–427

- Kumar J, Clayton CRI (2007) Effect of sample torsional stiffness on resonant column test results. *Can Geotech J* 44(2):221–230
- Leucci G, De Giorgi L (2006) Experimental studies on the effects of fracture on the P and S wave velocity propagation in sedimentary rock (“Calcarene del Salento”). *Eng Geol* 84:130–142
- Li JC, Ma GW (2009) Experimental study of stress wave propagation across a filled rock joint. *Int J Rock Mech Min Sci* 46(3):471–478
- Li JC, Ma GW, Zhao J (2010) An equivalent viscoelastic model for rock mass with parallel joints. *J Geophys Res* 115(B03305):1–10
- Perino A (2011) Wave propagation through discontinuous media in rock engineering. Ph.D. Thesis, Politecnico di Torino, Italy
- Perino A, Orta R, Barla G (2012) Wave propagation in discontinuous media by the scattering matrix method. *Rock Mech Rock Eng* 45(5):901–918
- Pyrak-Nolte LJ, Cook NGW (1987) Elastic interface waves along a fracture. *Geophys Res Lett* 14(11):1107–1110
- Pyrak-Nolte LJ, Myer LR, Cook NGW (1990a) Transmission of seismic waves across single natural fractures. *J Geophys Res* 95:8638–8671
- Pyrak-Nolte LJ, Myer LR, Cook NGW (1990b) Anisotropy in seismic velocities and amplitudes from multiple parallel fractures. *J Geophys Res* 95(B7):11345–11358
- Richart FE Jr, Hall JR, Woods RD (1970) *Vibration of soils and foundations*. Prentice Hall, Englewood Cliffs, NJ
- Schoenberg M (1980) Elastic wave behaviour across linear slip interfaces. *J Acoust Soc Am* 68(5):1516–1521
- Slawinski RA (1999) Finite-difference modeling of seismic wave propagation in fractured media. Ph.D. thesis, University of Calgary, Calgary